Scientific Research Publishing

Journal of Water Resource and Protection, 2025, 17(7), 504-529
https://www.scirp.org/journal/jwarp
ISSN Online: 1945-3108
ISSN Print: 1945-3094

Aerial Image Analysis of Changes in Wetlands between 2019 and 2023 in the Barataria and Breton Sound Basins of Coastal Louisiana

Christopher Potter

Earth Science Division, NASA Ames Research Center, Moffett Field, CA, USA
Email: chris.potter@nasa.gov

How to cite this paper: Potter, C. (2025) Aerial Image Analysis of Changes in Wetlands between 2019 and 2023 in the Barataria and Breton Sound Basins of Coastal Louisiana. *Journal of Water Resource and Protection*, **17**, 504-529.
https://doi.org/10.4236/jwarp.2025.177026

Received: April 5, 2025
Accepted: July 21, 2025
Published: July 24, 2025

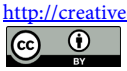

Abstract

Loss of marshlands in the Mississippi Delta plain of Louisiana threatens the future of the region's economy, one which is heavily reliant on coastal wetland resources. This study builds on previous remote sensing investigations over the Barataria and Breton Sound Basins to make increasingly detailed assessments of changes occurring in coastal wetlands of southern Louisiana from both human extractive activities and repeated hurricanes. We set out to answer two scientific questions: 1) What are the bio-geophysical nature and the areal extent of changes in coastal shorelines and wetlands of the Barataria and Breton Sound basins over the past four years of intensive hurricane activity? 2) How have marshland/water boundaries in the probable impact areas of the Mid-Barataria and Mid-Breton sediment diversions recently changed in the landscape of water and wetland-covered patches? High-resolution (<1-m pixel size) imagery, acquired and processed by the United States Department of Agriculture (USDA) National Agriculture Imagery Program (NAIP), was acquired from 2019 to 2023. Landscape metrics for ten equal-interval classes of NDWI were computed using the FRAGSTATS program. Class-level indices from FRAGSTATS were used to quantify the densities and spatial configuration of patches, providing a variety of metrics for the geometry, complexity, and aggregation levels of the wetland- versus water-covered patches across the study area. Analysis over the past four years (2019 to 2023) using the normalized difference water index (NDWI) from NAIP images revealed that there has been a widespread increase in relatively deep-water coverage (and corresponding losses of marshland coverage) since 2019 over most of the Barataria and Breton Sound Basins. Scouring of formerly shallow water cover and widespread erosion of brackish and fresh marshland shorelines followed the storm surges of Hurricanes Zeta (2020) and Ida (2021). There has been an extensive increase in relatively deep-water coverage (and corresponding losses of land

coverage) since 2019 over most of the marshlands and shorelines of the Barataria and Breton Sound Basins in southeastern Louisiana. Heightened fragmentation of marshland edges and interior pond features based on patch metric analysis implied that different types of damage inflicted on coastal wetlands of southeastern Louisiana from tropical storms can be characterized using aerial remote sensing.

Keywords

NAIP, NDWI, Southern Louisiana, Marshlands, Erosion, Tropical Storms

1. Introduction

Erosion of marshland soils and vegetation in Louisiana accounts for more than 80% of coastal wetland loss in the continental United States since the 1930s [1] [2]. Land loss threatens the future of the state's economy which is heavily dependent on coastally situated jobs in the fishing, hydrocarbon (oil and gas) extraction, and waterborne transportation industries. Slowing degradation along wetland margins on the Gulf of Mexico has been at the center of the state's response to protect and restore coastal communities in the face of future hurricane storm surges and sea level rise.

Subsidence in the Mississippi Delta plain has been mapped for decades [3]. Because sea level in the Gulf of Mexico is rising at rates not observed over the past several thousand years, it has been predicted that much of Delta land cover will be "drowned" in submergence events similar to those documented in the early Holocene [4].

Wave-driven erosion of wetlands is currently a primary physical mechanism for land loss in Louisiana's coastal estuaries [5], although a highly restricted sediment supply from the Mississippi River channel is the historical causal agent of regional wetland decline [6]. Tropical cyclone (hurricane) events have been shown to be highly destructive to coastal wetlands [7], but also can be a source of mineral sedimentation to organic marshes [8] [9]. In a recent survey report, Sharp (2021) [10] documented Hurricane Ida's impacts in August 2021 on the monitoring equipment and the marshlands at around 120 long-term monitoring sites in coastal Louisiana. Post-Ida site visits showed that roughly half of the sites were heavily damaged or completely destroyed by Ida's storm surge in the Barataria and Breton Sound Basins.

A significant compounding cause of wetland degradation has been canal cutting for oil and gas extraction since the 1940s, together with oil spills, such as the Deepwater Horizon (DWH) incident of April 2010 [1]. The DWH incident caused the largest marine oil spill in U.S. history, impacting the entire northern Gulf of Mexico ecosystem. Wetlands in the outer Barataria Basin estuary were the most heavily damaged by the persistence of toxic chemicals [11].

As part of Louisiana's comprehensive plan for coastal protection and restoration (CPRA, 2017 [1] and updated in 2023), the state now plans to spend several billion dollars constructing sediment diversions from the Mississippi River into both the Barataria and Breton Sound basins. Controlled sediment diversions offer a promising investment to re-establish hydrologic flows from the Mississippi River that carry land-building sediments to nourish marshlands and slow coastal land loss rates. The Mid-Barataria and Mid-Breton diversions, both to be located in Plaquemines Parish and constructed of earthen and concrete levees, will divert sediment-laden water from the Mississippi River and deposit it into the estuary basins to help rebuild, restore, and sustain marshlands [1].

To identify and characterize coastal wetland damage in the Breton Sound basin, Potter and Amer (2020) [2] utilized a multiband-subtraction methodology that calculates a Normalized Difference Water Index (NDWI) from Landsat-8 Operational Land Imager (OLI) images at 30-m pixel resolution. The NDWI was calculated from the blue and short-wave infrared bands and yielded land/water boundary maps. Landsat NDWI time-series analysis by Potter and Amer (2020) [2] estimated that 245 km^2 of wetlands in the Breton Sound Basin were transformed to open water from the impacts of Hurricanes Katrina and Gustav, equivalent to one-third the size of the city of New Orleans.

In the present study, high-resolution (<1-m pixel size) imagery, acquired and processed by the United States Department of Agriculture (USDA) National Agriculture Imagery Program (NAIP) from 2019 to 2023, was analyzed at the landscape scale to answer two scientific questions:

1) What are the bio-geophysical nature and the areal extent of changes in coastal shorelines and wetlands of the Barataria and Breton Sound basins over the past four years of intensive hurricane activity?

2) How have marshland/water boundaries in the probable impact areas of the Mid-Barataria and Mid-Breton sediment diversions recently changed in the landscape of water and wetland-covered patches?

The 6600 km^2 Barataria basin and its watersheds are located adjacent to the west bank of the Mississippi River in southeastern Louisiana and the Gulf of Mexico (**Figure 1**). The major water bodies of the basin include the northern freshwater Lac des Allemands, the mid-basin Lake Salvador and Little Lake, with Barataria Bay at the southern margin [12] [13]. Freshwater and sediment inputs to the Barataria Basin were largely eliminated by the construction of flood protection levees along the Mississippi River and the closure of Bayou Lafourche at Donaldsonville in the early 1900s. The southern half of the basin consists of tidally influenced marshes connected to a large bay system behind several barrier islands. The average water depth across this basin is 1.5 m and is normally unstratified. The subbasins most likely to be first impacted by the Mid-Barataria sediment diversion (MBASD) project will be Bayou Dupont, Bayou Grande Cheniere, and Round Lake [1] [14]. The tracts of both Hurricanes Zeta (October 2020) and Ida (August 2021) traversed the Barataria basin (**Figure 1**).

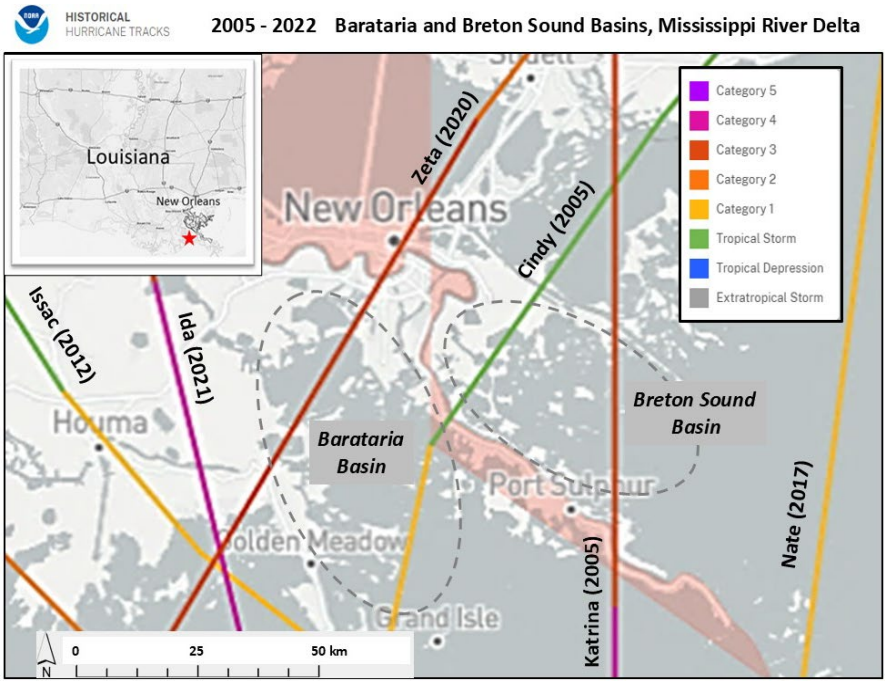

Figure 1. Hurricane paths making landfall in the Barataria and Breton Sound Basins of southeastern Louisiana from 2005 to 2022.

The Breton Sound basin in Plaquemines Parish spans 1880 km^2 from the eastern Mississippi River to the Mississippi River Gulf Outlet Canal, southeast of the city of New Orleans (Figure 1). Notable hydrologic features of the Breton Sound basin include Bayou Terre aux Boeufs and River aux Chenes, which are abandoned delta distributaries. Between 1940 and 1970, 33 km^2 of canals were dredged across the distributary ridges that run from the river to the outer fringes of the basin estuary [15], a disturbance which promoted elevated outflow of fresh water and increased saltwater intrusion. Subsidence combined with sediment deprivation from flood protection levees has contributed to marshland loss in the upper and middle basins, particularly in the Bohemia sub-basin. The sub-basins most likely to be first impacted by the Mid-Breton sediment diversion (MBRSD) project will be River aux Chenes and Spanish Lake [1]. The tracts of Hurricanes Zeta traversed the Breton Sound basin in October 2020 (Figure 1).

2. Methods

The data sources and processing methods for remote-sensing images used in this study are described in this section. Image analysis methods are described for NAIP data collected in the years 2019, 2021 and 2023, followed by methods of marshland gain and loss mapping results.

2.1. Land/Water Cover Index

The NAIP NDWI [16] was calculated from two surface reflectance bands using the equation:

$$\mathrm{NDWI} = (\mathrm{Green} - \mathrm{NIR})/(\mathrm{Green} + \mathrm{NIR}) \quad (1)$$

where, Green is the reflectance band from 0.53 to 0.59 μm, and NIR is the near-infrared reflectance band from 0.83 to 0.92 μm. The difference in land/water area (dNDWI) from one year to another was mapped for every major subbasin and estuary salinity zone inside the study area.

The NDWI values are a ratio that ranges from −1 to 1, with negative values indicating land that includes soil and live vegetation cover, and positive values indicating a majority of water coverage. If NDWI ranges from −1.0 to −0.2, then the pixel is 100% land, and if NDWI ranges from −0.2 to 0.0, then the pixel is a majority land and a minority water (Potter and Amer, 2020). If NDWI ranges from 0.0 to +0.49, then the pixel is a majority water and a minority land, and if NDWI ranges from +0.5 to +1.0, then the pixel is 100% water [16].

While there has been no spectral or atmospheric preprocessing of NAIP imagery regarding calibration across acquisition dates, the conversion of the RGB-NIR NAIP bands into a NDWI index effectively normalizes any spectral inconsistencies between image acquisition dates. A ratio of bands minimizes the absolute reflectance value differences between image acquisition dates and instead represents the NAIP pixel values in relative terms. Furthermore, atmospheric aerosol scattering effects in the NIR band region are weak, and consequently a time series of NDWI is less sensitive to atmospheric effects than is the normalized difference vegetation index (NDVI) [17].

The aircraft collecting different NAIP image data for this study would have passed over at different times of the day during the summer and autumn months, subjecting the images to subtle variations in tidal water levels along the lowest-lying areas of the Barataria and Breton Sound basins. The maximum daily tidal amplitude along the southeastern Louisiana coast is normally less than 20 cm [18], which would potentially introduce a higher level of uncertainty for pixels in the study area that were less than 15 cm elevation above sea level at any given hour and day. Because sea levels are rising in the Gulf of Mexico, the precise elevation relative to the sea level of any NAIP pixel area in the study region is a continuously changing variable over the four-year time period of this study.

2.2. Airborne Color-Infrared Imagery

Aerial image data were acquired from NAIP (www.fsa.usda.gov) as four-band imagery, composed of red, green, blue (RGB), and near-infrared (NIR) reflectance bands. Each NAIP image tile (DOQQ) covers a 3.7-minute quarter quadrangle.

NAIP image data acquired for the years 2019 (June-July), 2021 (November), and 2023 (June-July) were converted to NDWI raster images using Equation 1 for the Plaquemines Parish sections of the Barataria and Breton Sound basins. These NDWI products were regrouped into 10 equal-interval classes for subsequent statistical summaries. This processing step was taken to bin the NDWI values into broad classes of land/water cover and, as such, assure a high level of consistency between images collected on different dates.

2.3. Statistical Methods

Zonal statistics (including mean and standard deviation) for NDWI in each year were computed for the groups of NDWI class pixels that intersect selected a sub-basin polygon in a vector base layer created for the United States Geological Survey (USGS) Watershed Boundary Dataset (WBD). The hydrologic units (HU) in the WBD are arranged in a nested, 12-digit hierarchical system with each HU in the system identified using a unique code [19]. Any HU in the WBD defines the areal extent of surface water drainage to an outlet point on a dendritic stream network or to outlet points where the stream network is not dendritic.

To characterize the wetland plant species that occurred most frequently in each of the ten equal-interval classes for the NAIP NDWI mapped for the Plaquemines Parish sections of Barataria and Breton Sound basins, the point sampling dataset reported by Nyman *et al.* (2022) [20] was overlaid on the 2019 NDWI raster layer. Aerial surveys of wetland plant species were conducted in early 2021 from a helicopter in transects oriented in a north-south direction and spaced 3 km apart. Visual survey sites were located at a spacing of 0.8 km along these transects. Plant species present were identified, and their abundance was ranked by percent cover at each survey site. Based on species composition and abundance, each marsh survey station was also assigned a marsh type: fresh, intermediate, brackish, or saline marsh. For the present study, a 1-m polygon buffer zone around each marshland survey point was generated and used to calculate zonal statistics for 2019 NAIP NDWI values at a total of 1154 survey points.

2.4. Landscape Patch Metrics

Landscape metrics for the ten equal-interval classes of NDWI were computed using the FRAGSTATS program [21]. Class-level indices from FRAGSTATS were used to quantify the densities and spatial configuration of patches, providing a variety of metrics for the geometry, complexity, and aggregation levels of the wetland- versus water-covered patches across the study area.

The simplest index of landscape pattern is patch size. Patch size distribution can be summarized at the class level by a variety of metrics (e.g., mean, median, max and variance). The area-weighted mean patch size is also known as correlation length and indicates the distance that one might expect to traverse the map while staying in a particular patch, from a random starting point and moving in a random direction [22]. The boundaries between patches (or edges) represent another fundamental spatial attribute of a class mosaic. The most common measures of patch shape complexity are based fundamentally on the perimeter-to-area ratio (PARA).

The following landscape metrics for class area coverage and edge characteristics were compared for NDWI classes from 2019, 2021, and 2023 NAIP imagery: Percentage of landscape (PLAND), Area-weighted mean patch area (AREA_AM), Coefficient of variation in patch area (AREA_CV), Total edge (TE), Edge Density (ED). PLAND is a measure of how much of the landscape is comprised of a partic-

ular class. AREA_AM (m) provides a patch size metric as a function of the number of patches in the class and total class area. TE (m) is an absolute measure of total edge length of a particular patch type. ED (m ha-1) equals the sum of the lengths (m) of all edge segments in the landscape, divided by the total landscape area.

The following landscape metrics for patch shape characteristics were compared for NDWI classes from 2019, 2021, and 2023 NAIP imagery: GYRATE_AM is the area-weighted mean patch radius of gyration (m), which provides a measure of landscape continuity (also known as correlation length). This metric represents the average traversability of the landscape; specifically, the average distance one can move from a random starting point and traveling in a random direction without leaving the patch. CIRCLE is a shape metric that is computed as one minus patch area (m^2) divided by the area of the smallest circumscribing circle; this metric approaches 0 for circular patches and approaches 1 for elongated patches. SHAPE is the shape index metric and equals the patch perimeter (m) divided by the square root of patch area. SHAPE corrects for the size problem of the PARA index by adjusting for a square standard and, as a result, is the simplest and perhaps most straightforward measure of shape complexity. SHAPE approaches 1 when the patch is square and increases without limit as patch shape becomes more irregular.

Four representative sub-basin areas (7 km^2 each) were selected for FRAGSTATS analysis and visualization of wetland patch dynamics, two in probable impact areas of the Mid-Barataria sediment diversion and two in probable impact areas of the Mid-Breton sediment diversion (**Figure 2**; geographic coordinates provided in **Table 1**). The central locations of these sub-basins were selected on the basis of the presence of relatively continuous coverage of wetland vegetation in 2019 adjacent to named bayous, ponds, or lakes.

2.5. Water Level and Surface Elevation Monitoring Data

The state of Louisiana's Coastwide Reference Monitoring System (CRMS) has been designed to monitor the effectiveness of coastal restoration projects [23]. CRMS includes around 400 sites encompassing a range of fresh, intermediate, brackish, and salt marshes, monitored using standardized data collection techniques and fixed sampling schedules. The CRMS datasets for water level and land surface elevation were accessed and plotted for this study to compare to results for recent NAIP water/land class mapping.

Table 1. Sub-basins of the study area (covering 7 km^2 each) selected for FRAGSTATS analysis and visualization of wetland patch dynamics. Center locations of each circular sub-basin area are listed.

Sub-Basin Name	Diversion	Latitude	Longitude
Bayou McCutchen	Mid-Barataria	29.5798	−89.9443
Bayou Tambour	Mid-Barataria	29.5559	−89.9262
Little Oak Pond	Mid-Breton	29.6938	−89.9228
Lake Batola	Mid-Breton	29.6607	−89.8006

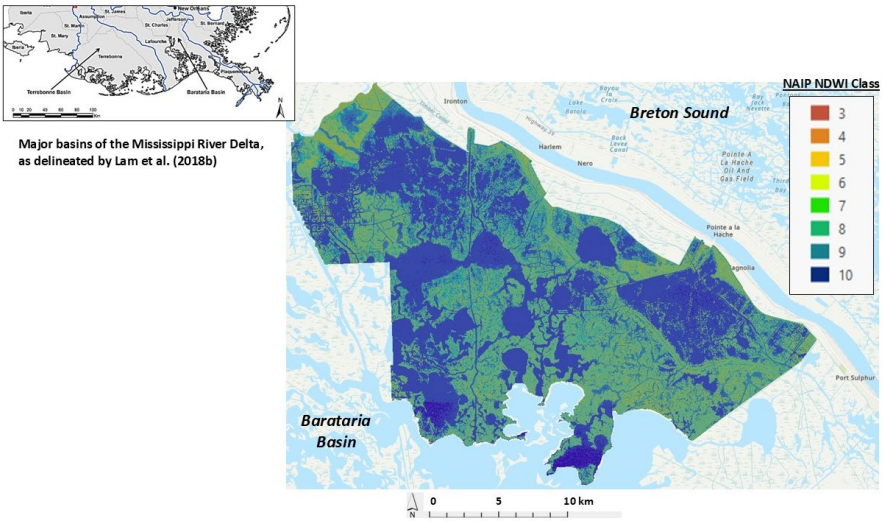

Figure 2. NDWI classes derived from 2019 NAIP imagery for the Barataria Basin portion of the study area.

The Rod Surface Elevation Table (RSET) method implemented within the CRMS network is used to estimate elevation change rates. One RSET benchmark is located at each CRMS site (with the exception of floating marshes and perpetually flooded, flocculent swamps). From the RSET benchmark, surface elevation is measured at nine points in four directions annually.

Surface elevation change is defined as cumulative elevation change since station establishment. For each sampling event, mean cumulative elevation change is calculated for each of the four directions, and an elevation change rate is estimated using linear regression of elevation change against time. The lines in this figure are linear regressions of elevation change (n = 4 per sample date) over time. Rates reported for elevation change are the slopes of the linear regression (cm yr^{-1}).

2.6. CRMS Monitoring Site Surveys after Hurricane Ida

In a recent survey report, Sharp (2021) [10] documented Hurricane Ida's impacts in August 2021 on the monitoring equipment and the marshlands at around 120 CRMS monitoring sites in coastal Louisiana. The photographic information on damage to marshlands assembled for these sites was compared to changes in NAIP NDWI from the 2019 and (post-Ida) 2021 image acquisitions in 100-m radius circular areas (0.3 km^2) centered on each reported station geolocation.

3. Results

3.1. Wetland Plant Cover in NWDI Classes

The frequency of plant species present across the entire study area in 2021, derived from the aerial survey sampling reported by Nyman *et al.* (2022) [20] overlaid on the 2019 NDWI raster layer (example in Figure 2), showed that the NDWI

class 4 (range of −0.2 to −0.4) had about 30% water cover (Table 2) and the highest frequency of freshwater-favoring marsh plants such as *Baccharis halimifolia*, *Colocasia esculenta, Phragmites australis*, *Sagittaria lancifolia*, and *Typha domingensis*. NDWI class 5 (range of 0.to −0.2) showed 63% water cover and was dominated by *Phragmites australis, Spartina alterniflora,* and *Spartina patens* in land cover areas. NDWI classes 6 and 7 (ranges of 0 to 0.2 and 0.2 to 0.4, respectively) both showed about 80% water cover and were dominated by brackish-favoring *Spartina alterniflora* and *Spartina patens* in land cover areas. NDWI

Table 2. Frequency of plant species present in NAIP NDWI classes, computed as the percent of sites reporting that species as the primary plant cover, based on the aerial survey sampling reported by Nyman *et al.* (2022) and overlaid on the 2019 NDWI raster layer of the Barataria and Breton Sound Basins.

NDWI 2019 Class	NDWI range	No. of Stations	Water	ALPH	AMAU	BACA	BAHA	CAHY3	CASE13	COES	CYPER	DISP	ECWA	FIMBR
3	0.4 to −0.6	2	0.0	0.0	0.0	0.0	0.0	0.0	0.0	50.0	0.0	0.0	0.0	0.0
4	0.2 to −0.4	59	30.5	1.7	1.7	0.0	1.7	0.0	0.0	6.8	3.4	0.0	3.4	0.0
5	0 to −0.2	349	63.3	0.9	0.0	0.0	0.3	0.0	0.3	0.9	0.6	0.3	0.3	0.3
6	0.2 to 0	156	81.4	1.3	0.6	0.0	0.0	0.0	0.0	0.6	0.6	0.6	0.6	0.0
7	0.4 to 0.2	64	79.7	1.6	3.1	0.0	0.0	1.6	0.0	0.0	0.0	0.0	0.0	0.0
8	0.6 to 0.4	108	97.2	0.0	0.0	0.0	0.0	0.0	0.0	0.0	0.0	0.0	0.0	0.0
9	0.8 to 0.6	331	98.2	0.0	0.0	0.3	0.0	0.0	0.0	0.0	0.0	0.0	0.0	0.0
10	1 to 0.8	85	100.0	0.0	0.0	0.0	0.0	0.0	0.0	0.0	0.0	0.0	0.0	0.0

HEAM	ISPA	JUEF	JURO	LUDWI	PHAU7	PLFO	POLYG4	SALA	SALA2	SALIX	SCAM6	SCHOE6	SCRO5	SPAL	SPPA	TYPHA	VILU3
0.0	0.0	0.0	0.0	50.0	0.0	0.0	0.0	0.0	0.0	0.0	0.0	0.0	0.0	0.0	0.0	0.0	0.0
0.0	0.0	0.0	0.0	0.0	37.3	0.0	0.0	11.9	0.0	0.0	1.7	0.0	1.7	0.0	6.8	10.2	0.0
0.3	0.3	0.3	1.4	0.3	18.9	0.3	2.0	6.9	0.3	0.6	1.1	0.3	1.4	10.6	17.8	4.6	1.7
0.0	0.0	0.0	3.2	0.6	7.1	0.0	0.0	1.3	1.3	0.0	0.6	0.0	1.3	25.0	19.2	0.6	0.0
0.0	0.0	0.0	0.0	0.0	9.4	0.0	0.0	1.6	0.0	0.0	3.1	0.0	0.0	3.1	12.5	1.6	4.7
0.0	0.0	0.0	0.0	0.0	0.9	0.0	0.9	0.9	0.0	0.0	0.0	0.0	0.0	3.7	8.3	0.0	0.0
0.0	0.0	0.0	0.3	0.0	1.2	0.0	0.0	0.0	0.0	0.0	0.0	0.0	0.0	1.5	1.8	0.0	0.0
0.0	0.0	0.0	0.0	0.0	0.0	0.0	0.0	0.0	0.0	0.0	0.0	0.0	0.0	2.4	3.5	0.0	0.0

Key to plant species in Table 2.

USDA Plant Symbol	Species	Common Name
ALPH	*Aletris farinosa*	white colicroot
AMAU	*Amaranthus tamaulipensis*	tamaulipas amaranth
BACA	*Bacopa caroliniana*	blue waterhyssop
BAHA	*Baccharis halimifolia*	groundsel bush sea-myrtle
CAHY3	*Calamagrostis hyperborea*	reed grass
CASE13	*Calystegia sepium*	hedge false bindweed
COES	*Colocasia esculenta*	coco yam
CYPER	*Cyperus* sp.	flatsedge
DISP	*Dichanthelium sphaerocarpon*	roundseed panicgrass
ECWA	*Echinochloa walteri*	coast cockspur grass
FIMBR	*Fimbristylis* sp.	fimbry
HEAM	*Helenium amarum*	sneezeweed
ISPA	*Isachne pallens*	bloodgreass
JUEF	*Juncus effusus*	common rush
JURO	*Juncus roemerianus*	needlegrass rush
LUDWI	*Ludwigia sp.*	primrose-willow
PHAU7	*Phragmites australis*	roseau cane
PLFO	*Pluchea foetida*	stinking camphorweed
POLYG4	*Polygonum sp.*	knotweed
SALA	*Sagittaria lancifolia*	bull tongue arrowhead
SALA2	*Sagittaria latifolia*	broadleaf arrowhead
SALIX	*Salix* sp.	willow
SCAM6	*Schoenoplectus americanus*	chairmaker's bulrush
SCHOE6	*Schoenoplectus* sp.	bulrush
SCOR5	*Scapania ornithopodioides*	bird's-foot earwort
SPAL	*Spartina alterniflora*	smooth cordgrass
SPPA	*Spartina patens*	saltmeadow cordgrass
TYPHA	*Typha domingensis*	southern cattail
VILU3	*Vigna luteola*	hairy cowpea
ZIMI	*Zizaniopsis miliacea*	giant cutgrass

classes 8, 9, and 10 (ranging from 0.4 to 1.0) showed greater than 90% water

cover and commonly less than 5% coverage by *Spartina* sp. or any other wetland plants.

The percent cover of pixels in NAIP images acquired in 2019, 2021, and 2023 for the Barataria Basin portion of the study area was compiled within NDWI equal-interval classes (Table 3) and showed that the greatest magnitude of change

Table 3. Percent cover of pixels in NAIP images from 2019, 2021, and 2023 within NDWI classes of the Barataria Basin of the study area. Coverage classes with the greatest magnitude of change are shaded in gray.

NDWI Class	NDWI range	2019 Percent	2021 Percent	2023 Percent
1	−0.8 to −1.0	0.002	0.002	0.003
2	−0.6 to −0.8	0	0	0
3	−0.4 to −0.6	0	0.001	0.063
4	−0.2 to −0.4	0.286	0.181	5.525
5	0 to −0.2	11.766	24.249	31.618
6	0.2 to 0	27.188	12.81	17.044
7	0.4 to 0.2	6.073	5.137	44.415
8	0.6 to 0.4	13.51	6.098	1.311
9	0.8 to 0.6	39.858	23.451	0.018
10	1 to 0.8	1.316	28.072	0.004

between 2019 and late 2021 (before and after the passage of both Hurricanes Zeta and Ida, respectively) was within NDWI class 5 (range of 0 to −0.2), which showed a 12% increase in marshland area dominated by *Phragmites australis* and *Juncus roemerianus,* and also within NDWI class 6 (range of 0 to 0.2), which showed a 16% decrease of marshland area dominated by *Spartina* sp. by late autumn of 2021. Within NDWI classes 8 and 9, which were relatively shallow water-dominated areas, these zones lost around 6% coverage between 2019 and 2021 and evidently contributed to a 27% increase in deeper water depth (NDWI class 10) coverage by late autumn of 2021, following Hurricanes Zeta (2020) and Ida (2021).

Changes in the percent cover of pixels in NAIP images of the Barataria Basin portion of the study area between late 2021 and mid-2023 showed that the greatest magnitude of change was within NDWI class 7 (range 0.2 to 0.4, 80% water cover) with sparse wetland cover dominated by brackish-favoring *Spartina* sp. This class 7 coverage increased by nearly 40% over the period since late 2021 (post-Hurricane Ida), whereas NDWI classes 8 - 10 each decreased to 1% or lower cover area in 2023. NDWI classes 5 class, co-dominated by *Phragmites australis* and *Spartina* sp., increased by 6% in area over the period since late 2021.

3.2. Comparisons of CRMS Monitoring Sites Following Hurricane Ida

Changes in NAIP NDWI from the 2019 (pre-Ida) and 2021 (post-Ida) image acquisitions at the (total of 85) CRMS sites photographed by Sharp (2021) [10] were

summarized in zonal statistics for 100-m radius circular areas (0.3 km^2) centered at each reported site (geo-location map in Figure 3). Comparison of frequency distribution plots (Figure 4) of the mean NDWI values for these 85 0.3 km^2 areas showed that the majority of sites shifted from mean values to the range NDWI of −0.2 to 0.2 in 2019 to a NDWI range of 0 to 0.4 in 2021, indicating a higher frequency of post-Ida water coverage. Comparison of frequency distribution plots (Figure 4) of the standard deviation of NDWI values for these 85 0.3 km^2 areas showed that the majority of sites shifted from values in the range of 0.25 to 0.35 in 2019 to a range of 0.35 to 0.45 in 2021, indicating a higher variability in post-Ida land versus water coverage.

Figure 3. Locations of CRMS stations (black dot symbols) surveyed by Sharp (2021) after the passage of Hurricane Ida in 2021. The station numbers were labeled for the four sites that showed the greatest change in mean NDWI from 2019 to 2021 NAIP image acquisitions.

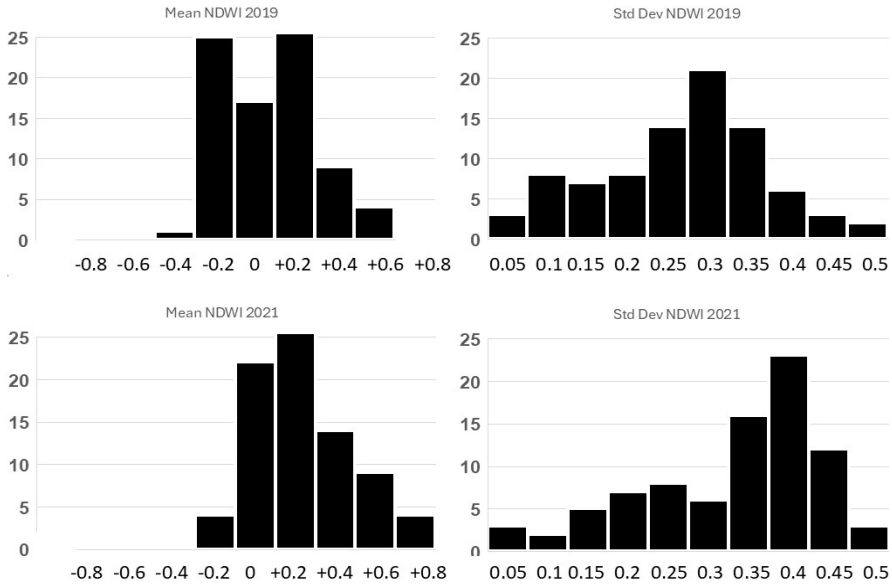

Figure 4. Frequency distribution plots of the mean and standard deviation of NAIP NDWI values for 0.3 km^2 areas (N = 85) centered on CRMS stations surveyed by Sharp (2021) before and after the passage of Hurricane Ida in 2021.

The four CRMS station sites that showed the greatest change in mean NDWI from 2019 to 2021 NAIP image acquisitions (labeled with station numbers in map Figure 3) were selected for comparisons to the photographic evidence of marshland change provided by Sharp (2021) [10]. The pre-Ida photos of these locations showed dense coverage of marshland vegetation surrounding the boardwalks and station pole markers at all four CRMS sites (Figure 5 and Figure 6), whereas post-Ida photos from Sharp (2021) [10] showed widespread removal of plant coverage and

Figure 5. Photographic evidence of marshland changes surveyed by Sharp (2021) before and after the passage of Hurricane Ida in 2021 at CRMS stations 115 and 161.

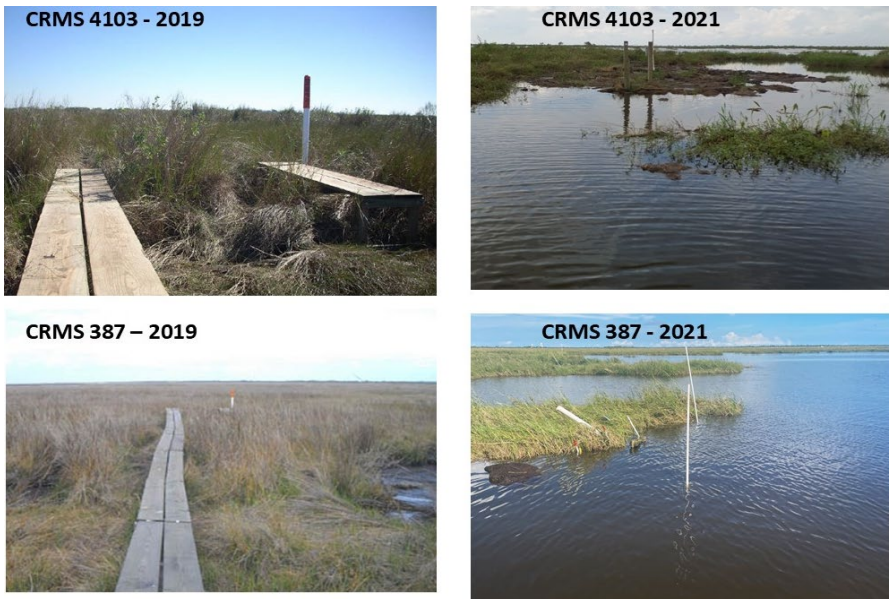

Figure 6. Photographic evidence of marshland changes surveyed by Sharp (2021) before and after the passage of Hurricane Ida in 2021 at CRMS stations 4013 and 387.

replacement by open water surrounding the station markers still remaining after the 2021 storm surge. The disturbance patterns revealed in these before- and after-Ida CRMS photographs verified that NAIP NDWI changes accurately quantified a higher frequency of post-Ida water coverage.

The 2019 to 2021 (post-Ida) NAIP NDWI map comparison at CRMS station 115 (Figure 7), located in the Spanish Lake sub-basin near the Pipeline Canal of inner Breton Sound Basin, showed extensive erosion of the vegetated marshland shoreline and transformation of NDWI class 5 (range of 0 to −0.2) dominated by *Phragmites australis* and *Spartina* sp. to NDWI class 8 open water coverage. Likewise, the 2019 to 2021 (post-Ida) NAIP NDWI map comparison at CRMS station 161 (Figure 7), located near the Raphael Pass sub-basin in the transition from Breton Sound Basin to the Chandaleur Sound, showed loss vegetated marshland, widening of several canals, large pond formations, and extensive transformation of NDWI classes 4 and 5 dominated by *Spartina* sp. to NDWI classes 8 to 10 open water coverage.

The 2019 to 2021 (post-Ida) NAIP NDWI map comparison at CRMS station 4103 (Figure 8), north of the Bayou Dupont sub-basin near a pipeline canal of inner Barataria Basin, showed deep erosion of all vegetated bayou shorelines, extensive pond formation and fragmentation of marshlands, and extensive transformation of most NDWI classes 4 and 5 coverage dominated by *Phragmites australis* and *Spartina* sp. to NDWI classes 8 and 9 open water coverage. The 2019 to 2021 (post-Ida) NAIP NDWI map comparison at CRMS stations 387 (sub-stations 1 and 2; Figure 8), located in the Grand Bayou Blue sub-basin of the Terrebonne Basin, showed nearly complete loss of vegetated marshland coverage, shoreline fragmentation, large pond formations, and extensive transformation of most NDWI classes 5 and 6 dominated by *Spartina* sp. to NDWI classes 9 to 10 open water coverage. These are now "plucked" marshlands that show numerous closely spaced, irregular scours and ponds [24].

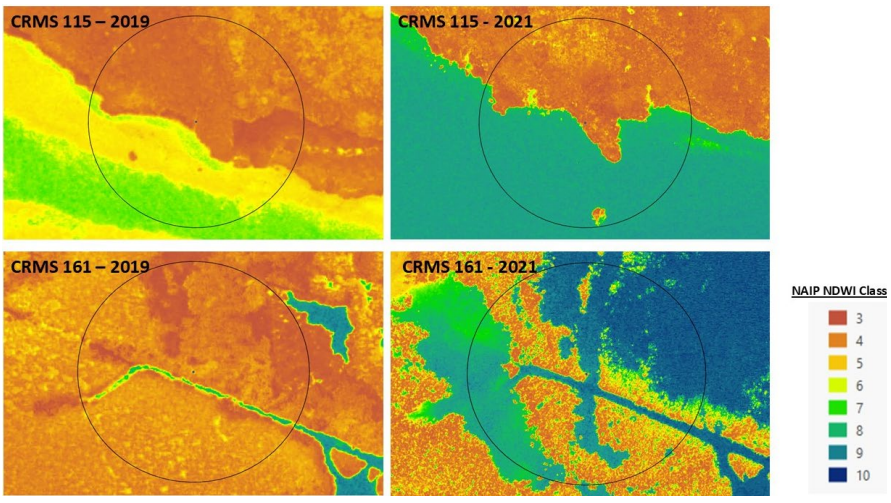

Figure 7. CRMS stations (115 and 161) areas that showed the greatest change in mean NDWI from 2019 to 2021 NAIP image acquisitions, with outlines of 100-m radius circular areas centered on the CRMS geo-location reported by Sharp (2021).

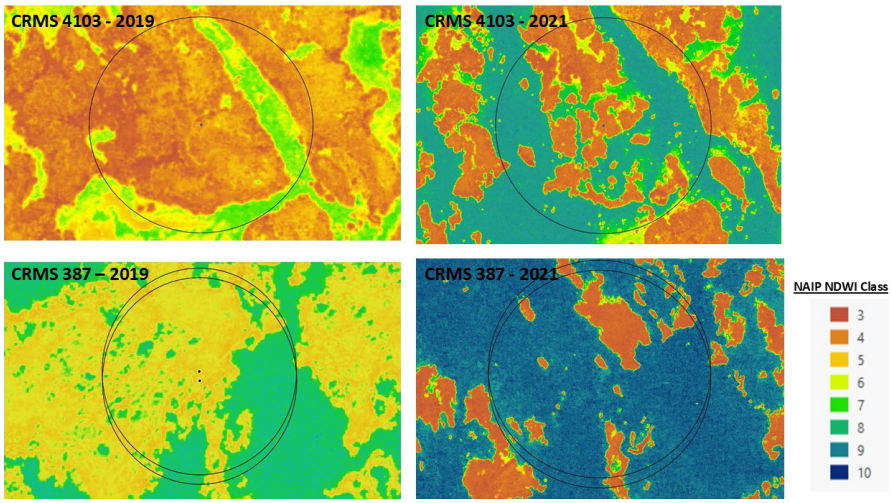

Figure 8. CRMS stations (4103 and 387) areas that showed the greatest change in mean NDWI from 2019 to 2021 NAIP image acquisitions, with outlines of 100-m radius circular areas centered on the CRMS geo-location reported by Sharp (2021).

3.3. Landscape Patch Dynamics in Sub-Basins

Analysis of the area cover and edge complexity of the wetland versus water-covered patches in probable impact areas of the Mid-Barataria and Mid-Breton sediment diversions was carried out for four circular 7 km^2 sub-basin areas, each with a diameter of 3 km (**Figure 9**). FRAGSTATS results (**Table 4**) showed that the NDWI class 4 (range of −0.2 to −0.4), dominated by freshwater-favoring marsh plants, had a PLAND of just 2.5% in 2019 and a relatively low AREA_AM of 1.4 m^2. In contrast, NDWI class 5 (range of 0 to −0.2), dominated by brackish-favoring marsh plants like *Spartina* sp., covered 15% of these sub-basin areas in 2019 and showed higher ED values along with an AREA_AM of 11 m^2. NDWI classes 6 - 8 (ranging from 0 to 0.6) and dominated by 80% - 90% water cover, covered 51% of these sub-basin areas in 2019 and showed the highest edge length (TE and ED) index values of all the NDWI classes. The AREA_AM coverage of these three classes ranged from 14 to 50 m^2 in 2019. NDWI class 9 covered 32% of these sub-basins in 2019 with an AREA_AM coverage of 253 m^2, whereas the (deepest) water class 10 covered less than 1% of these sub-basins in 2019.

FRAGSTATS analysis of the shape and connectivity levels of the wetland versus water-covered patches in probable impact areas of the Mid-Barataria and Mid-Breton sediment diversions (**Table 4**) showed that the GYRATE and SHAPE metrics increased with increasing water cover across the ten NDWI classes in 2019. A longer average traversability length and a more irregular overall shape in NDWI classes 7 - 9 patches were discovered, compared to classes 4 - 6 patches. The CIRCLE metric showed that NDWI classes 9 and 10 (deepest water cover) were those with the most circular (least irregular) patch shapes in 2019.

Between 2019 and 2021 NAIP image acquisitions, several notable changes were detected in the landscape metrics for NDWI classes in these same four 7 km^2 sub-basins. The most striking shift was in the percent cover (PLAND) and AREA_AM

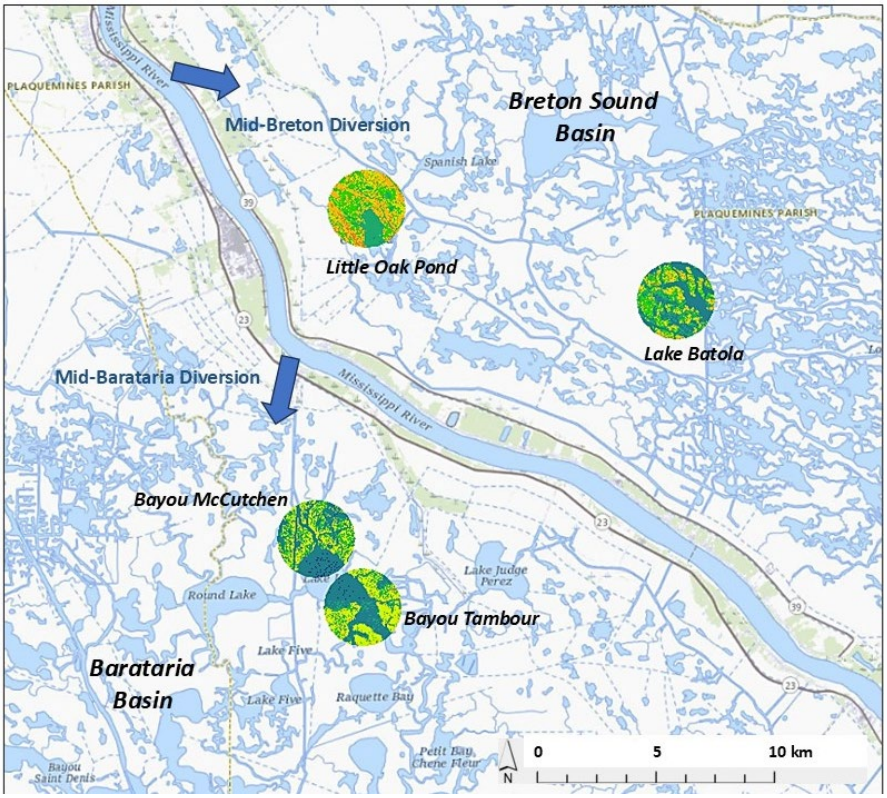

Figure 9. Locations of four sub-basins used in landscape patch analysis for the Barataria and Breton Sound Basins.

Table 4. (a) Landscape patch metrics from NAIP image analysis from the years 2019, 2021, and 2023 within NDWI classes of the four sub-basin areas shown in Figure 3. Column headings are defined as follows: Percentage of landscape (PLAND; %), Total edge (TE; m), Edge Density (ED; m ha^{-1}), Area-weighted mean patch area (AREA_AM; m^2), Coefficient of variation in patch area (AREA_CV). (b) Column headings are defined as follows: Area-weighted mean patch radius of gyration or the average traversability of the landscape (GYRATE_AM; m); Shape index (SHAPE), Circular shape index (CIRCLE).

(a)

2019 NDWI Class	PLAND	TE	ED	AREA_AM	AREA_CV
3	-	2	0	0	0
4	2.5	660201	237.1	1.382	2674
5	14.6	2328773	836.3	10.919	4648
6	17.6	3565343	1280.4	13.539	3817
7	16	3526448	1266.4	50.098	8486
8	17.2	3793353	1362.2	32.397	11388
9	31.5	2608909	936.9	253.053	13628
10	0.5	450041	161.6	0.001	158
2021 NDWI Class	PLAND	TE	ED	AREA_AM	AREA_CV
3	0	92	0	0	41
4	0.4	198147	71.2	0.069	1146
5	19.1	2972343	1067.4	8.092	2715
6	6.9	3778960	1357	0.141	1306

Continued

7	5.1	2302023	826.7	0.595	2737
8	5.1	2253466	809.2	0.332	1857
9	31.6	8711400	3128.3	126.211	22135
10	31.8	7482321	2686.9	210.641	22114
2023 NDWI Class	PLAND	TE	ED	AREA_AM	AREA_CV
1	0	7	0	-	-
2	0	146	0	-	17
3	0	21451	0.7	0	58
4	6.4	3749644	119.7	0.888	4075
5	28.5	6695021	213.6	31.449	7939
6	23.2	6428726	205.1	40.295	18643
7	41.4	4090545	130.5	236.613	15267
8	0.5	730764	23.3	0	59
9	0	9800	0.3	-	17
10	0	334	0	-	16

(b)

2019 NDWI Class	GYRATE_AM	GYRATE_CV	SHAPE_AM	SHAPE_CV	CIRCLE_AM	CIRCLE_CV
3	0.3	0	1	0	0	0
4	48.2	259.9	9	45.03	0.75	68.97
5	174.9	433.9	20.9	57.88	0.79	65.93
6	180.5	452.5	34	112.45	0.78	66.34
7	320.2	338	39.3	95.63	0.8	60.58
8	259.4	452.5	29.7	60.75	0.78	78.24
9	852.7	856.3	84.7	68.47	0.62	76.19
10	1	69.7	1.4	18.13	0.56	93.56
2021 NDWI Class	GYRATE_AM	GYRATE_CV	SHAPE_AM	SHAPE_CV	CIRCLE_AM	CIRCLE_CV
3	0.54	10.2	1	6.99	0.12	311.18
4	9.7	134.2	4.1	38.4	0.62	140.53
5	167.81	451.4	24.5	90.26	0.78	86.33
6	14.68	145.4	6.4	52.97	0.71	86.69
7	28.71	188.5	8.4	45.75	0.7	105.84
8	28.04	226.4	7.6	51.55	0.74	107.49
9	600.44	383	157.2	82.47	0.73	108.96
10	642.76	399.9	162.4	103.78	0.58	101.16
2023 NDWI Class	GYRATE_AM	GYRATE_CV	SHAPE_AM	SHAPE_CV	CIRCLE_AM	CIRCLE_CV
1	0.3	-	1	-	-	-
2	0.3	-	1	-	0.03	538.52
3	0.3	17.9	1	5.67	0.23	179.09

Continued

4	37.3	208.9	13.2	52.8	0.74	76.13
5	258	527	58.1	110.34	0.76	76.61
6	316.5	450.1	55.1	51.43	0.8	92.02
7	714.7	838.2	106.5	76.29	0.6	80.69
8	0.4	22.9	1.1	9.32	0.3	149.68
9	0.3	2.3	1	1.44	0.03	588.7
10	0.3	-	1	-	0.03	576.63

of shallow water-dominated NDWI classes 6 - 8 that transitioned into relatively large patches of deeper water-dominated classes 9 and 10 (Table 4). In addition, the TE and ED values of NDWI classes 9 and 10 increased by several-fold between 2019 and 2021, suggesting that longer, more complex shorelines and marshland edge boundaries were developed with classes 5 and 6. The reduction of the GYRATE and SHAPE metric values across all NDWI classes 4 - 9 between 2019 and 2021 further suggested that more compact, less irregular patch shapes of both wetland and water cover were formed during the years 2020 and 2021 in the four sub-basins areas. The CIRCLE metric increased noticeably for all NDWI classes implying more circular (and less irregular) patch shapes were formed in these sub-basins between 2019 and 2021.

Between NAIP image acquisitions in 2021 (post-Hurricane Ida) and in 2023, several noteworthy changes were detected in the landscape metrics for NDWI classes in these same four sub-basins. A distinct shift occurred in the percent cover (PLAND) and AREA_AM of deep water-dominated NDWI classes 9 and 10, transitioning into large patches of relatively shallow water-dominated classes 5 - 7 (Table 4). In addition, the TE and ED values of NDWI classes 9 and 10 decreased considerably between 2021 and 2023, transitioning to the longest, most complex shorelines and marshland edge boundaries in NDWI classes 5 - 7. Associated increases in the GYRATE and SHAPE metric values cross NDWI classes 5 - 7 further suggested that less compact, more irregular patch shapes of wetland cover were formed in the four sub-basins areas between 2021 and 2023. The CIRCLE metric decreased markedly for NDWI classes 8 - 10 (predominantly water cover), implying less circular (and more irregular) patch shapes by 2023 for the deepest water cover zones.

Mapping of NAIP NDWI classes in these four 7 km^2 sub-basins over time revealed numerous locations where shoreline erosion and/or wetland drowning have occurred (Figure 10). Extensive shoreline erosion was detected between 2019 and 2021 on the southern margins of the Bayou McCutchen sub-basin and in the center of the Bayou Tambour sub-basin. In the Breton Sound sub-basin areas of Little Oak Pond and Lake Batola, replacement of NDWI class 6 (partially vegetated) marshland patches detected in 2019 by NDWI class 9 and 10 open water cover was extensive by 2021.

Patterns of change between 2019 and 2021 in NDWI classes 7 – 10 could be seen in these four 7 km^2 sub-basins, most prominently in the shift from a predominance of shallow water depths to deeper water depths in all sub-basin examples. The absence of smooth gradations from NDWI class 7 to class 8 that were evident in 2019 NAIP images, instead showing deeper NDWI class 9 and 10 areas in 2021 NAIP imagery in these buffer zones adjacent to patches of marshland plants.

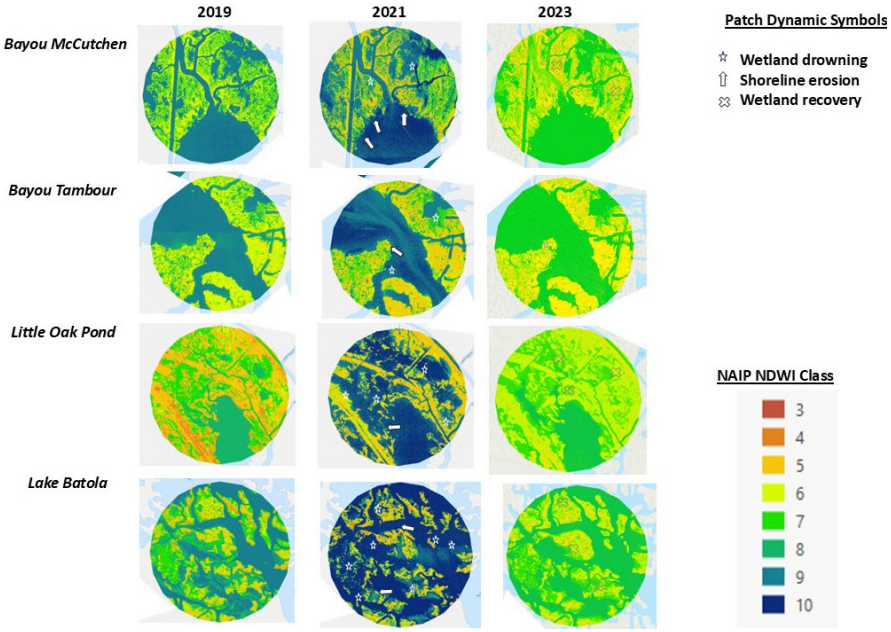

Figure 10. Maps of NDWI classes within four sub-basins in the Barataria and Breton Sound Basins, from NAIP imagery collected in 2019, 2021, and 2023.

The changes in patch geometry between 2021 (post-Hurricanes Zeta and Ida) and 2023 in NDWI classes could be seen most prominently in the shift from a predominance of relatively deep-water depths to shallower water depths and a widespread recovery of NDWI class 7 (80% water cover) with sparse wetland cover dominated by brackish-favoring *Spartina* sp. Patches of NDWI classes 4 and 5, dominated by *Phragmites australis* and *Juncus roemerianus* in 2019 NAIP imagery, have failed to recover and regrow extensively since 2021 in these four sub-basins (**Figure 10**).

Spatial variability in patch metrics, as measured by the coefficient of variation (CV; **Table 4**), increased for the AREA_AM, SHAPE_AM, and CIRCLE_AM metrics of NDWI classes 9 and 10 between 2019 and 2021. Variability in the patch metrics AREA_AM, GYRATE_AM, and SHAPE_AM of NDWI classes 5 - 7 increased by several-fold between 2021 and 2023.

3.4. Measured Water and Surface Elevation Changes at CRMS Stations

Plots of water elevation change (**Figure 11** from the CRMS data viewer) from the closest CRMS station locations to the four sub-basins in the Barataria and Breton

Sound Basins (shown in Figure 9) all showed a substantial rise in water levels immediately following both Hurricane Zeta (2020) and Hurricane Ida (2021).

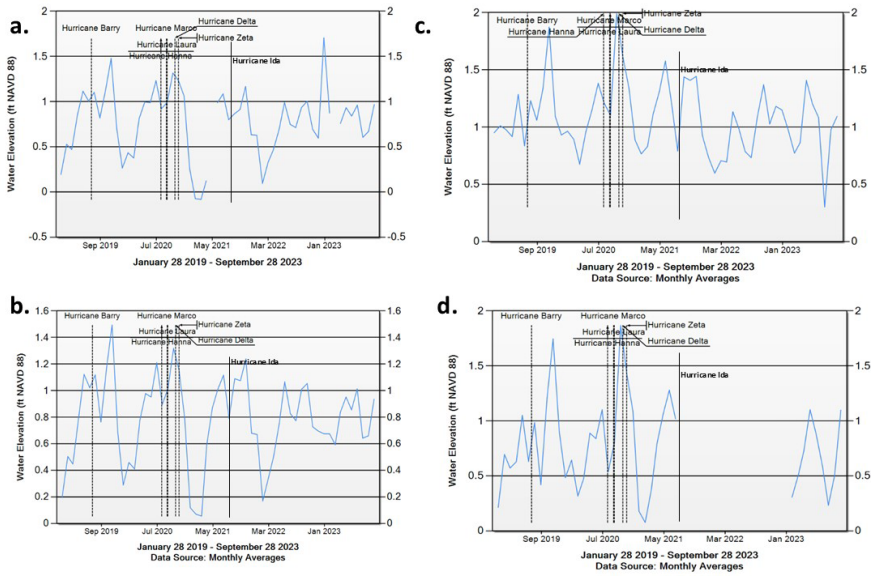

Figure 11. Plots of water elevation change from the closest Coastwide Reference Monitoring System (CRMS) station locations to the four sub-basins in the Barataria and Breton Sound Basins shown in Figure 2. (a) Bayou McCutchen, (b) Bayou Tambour, (c) Little Oak Pond, (d) Lake Batola. Conversion factor is 1 foot equals 30.5 cm of water level change.

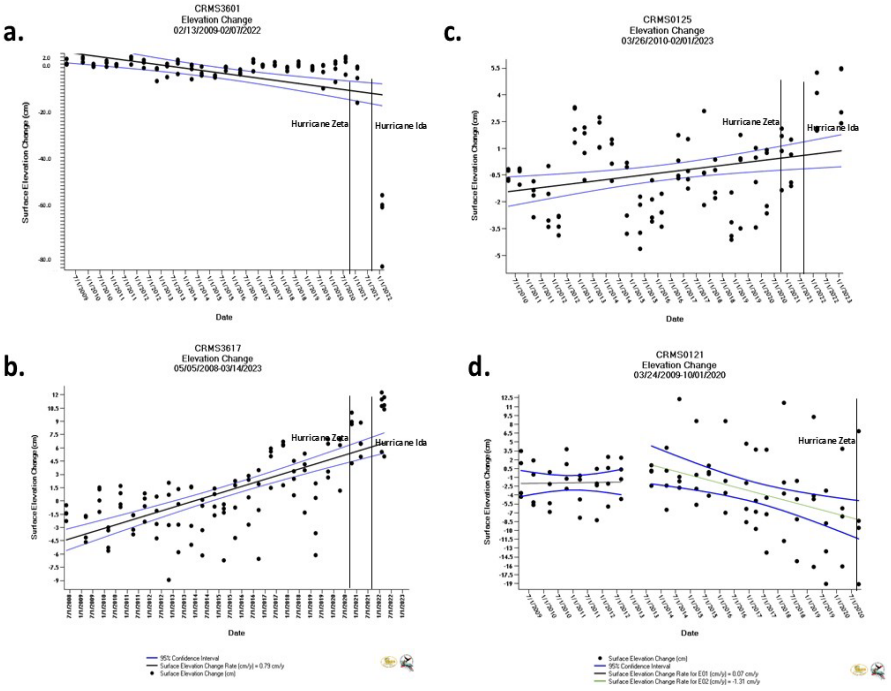

Figure 12. Plots of land elevation change from the closest Coastwide Reference Monitoring System (CRMS) station locations to the four sub-basins in the Barataria and Breton Sound Basins shown in Figure 2. (a) Bayou McCutchen, (b) Bayou Tambour, (c) Little Oak Pond, (d) Lake Batola CRMS monitoring equipment nearest the Lake Batola sub-basin was evidently disabled after the passage of Hurricane Ida in August 2021.

In general, the water elevation at all four stations reached peak measured change levels of 5 to 15 cm over the time period between 2019 and 2023 immediately following these intense storm surges. Water elevation dropped by around 5 cm over the years 2022 - 2023 at all four stations. This difference in water levels after the two hurricanes in 2020 and 2021 verified that the shift from NDWI class 6 and 7 to classes 9 - 10 was associated with deeper water depths detected by NAIP images. It is worth noting that the monitoring equipment nearest the Lake Batola sub-basin was evidently disabled for around 16 months after the passage of Hurricane Ida.

Plots of land surface elevation change (**Figure 12** from the CRMS data viewer) from the closest CRMS station locations to the four sub-basins in the Barataria and Breton Sound Basins (shown in **Figure 9**) displayed more diverse patterns. The CRMS stations closest to the Bayou McCutchen and Lake Batola sub-basins both showed steep negative trends in land elevation levels (and apparent wetland drowning) following Hurricane Zeta, whereas land elevation trends at the stations closest to the Bayou Tambour and Little Oak Pond sub-basins showed minor declines in land elevation following Hurricane Zeta and Hurricane Ida.

4. Discussion

The main findings from this study were that there has been an extensive increase in relatively deep-water coverage (and corresponding losses of land coverage) since 2019 over most of the marshlands and shorelines of the Barataria and Breton Sound Basins in southeastern Louisiana. Deep scouring and widespread erosion of brackish and fresh marshlands were detected after Hurricane Ida in 2021 NAIP imagery [24]. In the Barataria Basin, the combined impacts of the DWH Oil Spill in 2010 [11], Hurricane Zeta in 2020, and Hurricane Ida in 2021, whose eye traveled just west of Bayou Lafourche on the western margins of the Basin, eroded the estuary into progressively larger patches of deeper water cover. Longer shorelines and marshland edge boundaries were developed, particularly in brackish marsh cover areas. In the Breton Sound Basin, the storm surge of Hurricane Zeta in 2020 resulted in widespread drowning of both freshwater and brackish marsh vegetation cover and generated more compact, less irregular patch shapes of both wetland and water cover. Many square kilometers of sparsely vegetated marshland patches dominated by *Spartina* sp. that were mapped in 2019 were replaced by open water cover following the storm surge of Hurricane Ida in August 2021.

Spatial variability in the patch metrics for area coverage and irregularity of shapes increased in deeper-water areas mapped by NAIP imagery between 2019 and 2021 in the Barataria and Breton Sound Basin study areas. Variability in the patch attributes of sparsely wetland-covered areas increased markedly between 2021 (post-Ida) and 2023, suggesting that there is presently a more fragmented landscape of regrowing marshland patches dominated by *Spartina* sp. than was present in 2019.

Hurricanes have been documented to damage marsh plants and reduce wetland

biomass production which is essential for organic accretion in coastal zones [24] Tropical storm surges may decrease marsh elevation by removing substrates near the shoreline and channel edges through scouring and erosion [25], or conversely, intense storms can increase marsh elevation by moving sediment onto tidal flats [8] [9].

In the survey report by Sharp (2021) [10], photographic evidence revealed uprooting and nearly complete drowning of marsh plant cover at damaged Barataria Basin CRMS stations following Hurricane Ida. Some sites in Breton Sound appeared to be "salt burned", meaning that saline water introduced into freshwater marsh zones from the storm surge killed much of the vegetation cover. Stations in the Mississippi River bird's-foot Delta facing Chandaleur Sound commonly saw washed-up wrack (dead reeds and leaf debris mixed with trash) and sediment deposits. This photographic evidence of wetland loss was consistent with the mapping of NDWI class dynamics from NAIP imagery collected in 2019 (pre-Ida) and 2021 (post-Ida).

In previous studies of wetland fragmentation processes, Lam *et al.* (2018) [26] weak regression results between fragmentation and wetland loss in the Mississippi River Delta plain, with R^2 values between 0.20 and 0.45. These authors suggested that additional factors needed to be considered in such fragmentation studies, including (1) testing with different land/water ratio thresholds; (2) elevation effects; (3) distance to the coast, and (4) storm surge effects. In a more conclusive study, Stagg *et al.* (2020) [27] reported differences in the landscape configuration of vegetated and open water pixels in healthy and degrading wetlands of the Chenier Plain along the Northern Gulf of Mexico. Healthy wetlands were more aggregated, and degrading wetlands were more fragmented. Greater aggregation levels were associated with higher wetland elevation and better drainage, compared to fragmented wetlands, at lower elevations and poorer drainage.

To further compare how changes in marshland versus open water cover from the present study align with or differ from trends observed in past published studies in the Mississippi River Delta region, Potter (2021) [10] reported for subbasins of the western Barataria Basin near the Bayou Lafourche that, based on trends in Landsat NDWI, a baseline total of 42.3 km^2 was estimated to fall into the category of wetland loss since 2005. The leading subbasins for these recent wetland-to-water conversions made up most of the southwestern portion of the study area just north of Port Fourchon. Potter and Sukanna (2024) [28] used Landsat NDWI to map the extensive erosion of marshland edges in northern Barataria Bay that has continued from 2013 to 2022. Oiling from the Deepwater Horizon spill event in 2010 has contributed to high erosion rates observed after recent tropical storms in 2020 and 2021 in Barataria Bay. These authors concluded that the combination of Landsat NDWI trend mapping with high-resolution image segmentation of marshland edges and interior features confirms that different types of biophysical damage inflicted on coastal wetlands of southeastern Louisiana from tropical storms can be characterized using this combination of satellite and aerial remote

sensing.

As a general overview of wetland disturbance processes in the Mississippi River Delta region, interior marsh pond formation and enlargement, either elongated or irregular in shape, can result from erosion on pond perimeters, flooding of wetlands within a pond, and coalescing of adjacent ponds [29]. Expansion of open water area is often not uniform around an interior pond perimeter, and wetland loss often occurs on a margin that is impacted most by the direction of the wind-driven waves. Coastal Louisiana is a micro-tidal system and the waves interacting with the marsh edges are generated locally within a shallow bay with minimal river current influence [6].

In storm-impacted coastal areas, "plucked" marshlands [24] show numerous small, closely spaced, circular or irregular scours or ponds that are distributed over a wide area, resulting in a pockmarked appearance [30]. Laterally displaced marsh mats and marsh balls can be formed from deep scouring and erosion of brackish and fresh marshlands that commonly form elongated strips or disaggregated clumps of organic matter [24]. High-resolution (<1 m pixel size) aerial imaging such as that from 2021 NAIP data readily resolved and identified such clumps and mats of organic debris in plucked marshlands at CRMS station numbers 4103 and 387.

Marsh collapse and drowning can occur if ponds in the wetlands zone enter a runaway expansion phase [29]. Runaway expansion may occur when ponds are greater than a critical width because edge erosion by waves increases the fetch (pond width), which can feed back to elevate the wave size and further increase marsh edge erosion [30] [31]. However, Mariotti (2016) [30] reported that connected ponds in Terrebonne Bay (just west of the Barataria Basin) were expanding even if their diameter was only 10 - 50 m, suggesting that a threshold width for runaway wave erosion is not well understood. Mariotti (2016) [29] went on to predict that connected ponds of any size would expand if critical inorganic deposition rates were smaller than the rate of sea level rise, a condition common in marshlands of the Mississippi Delta region. High-resolution aerial imaging should readily identify and measure the changes in the areas of small marshland ponds, down to a few square meters coverage.

Marsh edge erosion studies by Sapkota and White (2019) [6] in the Barataria Basin, near the sites measured by Deis *et al.* (2019) [32] as well, implied that variability in erosion rates, measured at between 0.5 and 3.5 m yr^{-1}, was attributed to wind duration and soil bulk density and organic matter content. Marsh edges adjacent to the open bay experienced greater erosion rates than the protected sites located adjacent to the shallow water bodies in the northern part of the basin. This difference was attributed to the long fetch of unprotected sites, in contrast to shallow bathymetry in more protected sites and small fetches that produce waves with relatively low power. These edge erosion rates from 2017-2018 reported by Sapkota and White (2019) [6] were somewhat lower than the range of (DWH oiled) shoreline erosion rates (at between 2 and 5 m yr^{-1}) measured by Deis *et al.* (2019)

[32] following Hurricane Katrina and the DWH oil spill and mapped at 1-m resolution.

To summarize, aerial remote sensing of hurricane impacts on coastal wetlands can be used to support decision-making processes, such as prioritizing restoration efforts, monitoring the effectiveness of management actions, and assessing the long-term resilience of coastal wetlands to climate change. When individual marshland plant species can be identified and mapped every year over the Mississippi River Delta plain for changes in abundance, better-informed decisions can be formulated about how to remediate areas that are heavily disturbed by intensive hurricane storm surges.

5. Conclusion

This study expanded on remote sensing data collected by satellites over the Barataria and Breton Sound Basins to make increasingly detailed assessments of changes occurring in coastal wetlands of southern Louisiana. Analysis over the past four years (2019 to 2023) using NDWI from NAIP image acquisitions showed that there has been a widespread increase in relatively deep-water coverage (and corresponding losses of land coverage) since 2019 over most of the marshlands and shorelines of the basins. This has evidently resulted from deep scouring and widespread erosion of brackish and fresh marshlands following the storm surges of recent hurricanes in 2020 and 2021. Accelerated fragmentation of shoreline edges and interior pond features indicates that different types of damage inflicted on coastal wetlands of southeastern Louisiana from tropical storms can be characterized using aerial remote sensing.

Data Availability

The datasets generated during the current study are available from the corresponding author on reasonable request.

Conflicts of Interest

The author declares no conflicts of interest regarding the publication of this paper.

References

[1] Coastal Protection and Restoration Authority (CPRA) (2017) Louisiana's Com-Prehensive Master Plan for a Sustainable Coast. 184 p.

[2] Potter, C. and Amer, R. (2020) Mapping 30 Years of Change in the Marshlands of Breton Sound Basin (Southeastern Louisiana, U.S.A.): Coastal Land Area and Vegetation Green Cover. *Journal of Coastal Research*, **36**, 437-450. https://doi.org/10.2112/jcoastres-d-19-00174.1

[3] González, J.L. and Tornqvist, T.E. (2006) Coastal Louisiana in Crisis: Subsidence or Sea Level Rise? *Eos, Transactions American Geophysical Union*, **87**, 493-498. https://doi.org/10.1029/2006eo450001

[4] Blum, M.D. and Roberts, H.H. (2009) Drowning of the Mississippi Delta Due to In-

sufficient Sediment Supply and Global Sea-Level Rise. *Nature Geoscience*, **2**, 488-491. https://doi.org/10.1038/ngeo553

[5] Wilson, C.A. and Allison, M.A. (2008) An Equilibrium Profile Model for Retreating Marsh Shorelines in Southeast Louisiana. *Estuarine, Coastal and Shelf Science*, **80**, 483-494. https://doi.org/10.1016/j.ecss.2008.09.004

[6] Sapkota, Y. and White, J.R. (2019) Marsh Edge Erosion and Associated Carbon Dynamics in Coastal Louisiana: A Proxy for Future Wetland-Dominated Coastlines World-Wide. *Estuarine, Coastal and Shelf Science*, **226**, Article 106289. https://doi.org/10.1016/j.ecss.2019.106289

[7] Hauser, S., Meixler, M.S. and Laba, M. (2015) Quantification of Impacts and Ecosystem Services Loss in New Jersey Coastal Wetlands Due to Hurricane Sandy Storm Surge. *Wetlands*, **35**, 1137-1148. https://doi.org/10.1007/s13157-015-0701-z

[8] Turner, R.E., Baustian, J.J., Swenson, E.M. and Spicer, J.S. (2006) Wetland Sedimentation from Hurricanes Katrina and Rita. *Science*, **314**, 449-452. https://doi.org/10.1126/science.1129116

[9] Tweel, A.W. and Turner, R.E. (2012) Landscape-Scale Analysis of Wetland Sediment Deposition from Four Tropical Cyclone Events. *PLOS ONE*, **7**, e50528. https://doi.org/10.1371/journal.pone.0050528

[10] Sharp, L.A. (2021) Hurricane Ida Impacts to Coastwide Reference Monitoring System (CRMS) Sites. Coastal Protection and Restoration Authority, Mid-Basin Sediment Diversion Program, Coastwide Reference Monitoring System (CRMS). https://coastal.la.gov/wp-content/uploads/2021/11/CPRA-board-Post-Ida-11-17-21-Leigh-Anne-Share.pdf

[11] McClenachan, G. and Turner, R.E. (2023) Disturbance Legacies and Shifting Trajectories: Marsh Soil Strength and Shoreline Erosion a Decade after the Deepwater Horizon Oil Spill. *Environmental Pollution*, **322**, Article 121151. https://doi.org/10.1016/j.envpol.2023.121151

[12] Potter, C. (2021) Remote Sensing of Wetland Area Loss and Gain in the Western Barataria Basin (Louisiana, U.S.A.) since Hurricane Katrina. *Journal of Coastal Research*, **37**, 953-963. https://doi.org/10.2112/jcoastres-d-20-00119.1

[13] Potter, C. (2022) Application of Landsat 8 Aquatic Reflectance Band Data to Analyze Variations in Chlorophyll A, Suspended Sediment, N, and P in Coastal Estuaries of Southern Louisiana. *Journal of Remote Sensing and GIS*, **12**, Article 1000271.

[14] Trustee Implementation Group (TIG) (2022) Mid-Barataria Sediment Diversion Final Phase II Restoration Plan #3.2. 1123 p.

[15] Gagliano, S.M., Kwon, H.J. and van Beek, J.L. (1970) Deterioration and Restoration of Coastal Wetlands. *Proceedings of the* 12*th International Conference on Coastal Engineering*, Washington, 1967-1981.

[16] Amer, R., Kolker, A.S. and Muscietta, A. (2017) Propensity for Erosion and Deposition in a Deltaic Wetland Complex: Implications for River Management and Coastal Restoration. *Remote Sensing of Environment*, **199**, 39-50. https://doi.org/10.1016/j.rse.2017.06.030

[17] Gao, B. (1996) NDWI—A Normalized Difference Water Index for Remote Sensing of Vegetation Liquid Water from Space. *Remote Sensing of Environment*, **58**, 257-266. https://doi.org/10.1016/s0034-4257(96)00067-3

[18] Schoolmaster, D.R., Stagg, C.L., Sharp, L.A., McGinnis, T.E., Wood, B. and Piazza, S.C. (2018) Vegetation Cover, Tidal Amplitude and Land Area Predict Short-Term Marsh Vulnerability in Coastal Louisiana. *Ecosystems*, **21**, 1335-1347.

https://doi.org/10.1007/s10021-018-0223-7

[19] Jones, K., Niknami, L., Buto, S. and Decker, D. (2022) Federal Standards and Procedures for the National Watershed Boundary Dataset (WBD): Chapter 3 of Section A, Federal Standards, Book 11, Collection and Delineation of Spatial Data. Utah Water Science Center, 54 p.

[20] Nyman, J.A., Reid, C.S., Sasser, C.E., Linscombe, J., Hartley, S.B., Couvillion, B.R., and Villani, R.K. (2022) Vegetation Types in Coastal Louisiana in 2021 (ver. 2.0, April 2023). US Geological Survey Data Release.

[21] McGarigal, K., Cushman, S.A., Neel, M.C. and Ene, E. (2002) FRAGSTATS: Spatial Pattern Analysis Program for Categorical Maps. University of Massachusetts. https://www.umass.edu/landeco/research/fragstats/fragstats.html

[22] Keitt, T., Urban, D.L. and Milne, B.T. (1997) Detecting Critical Scales in Fragmented Landscapes. *Conservation Ecology*, **1**, Article 4. https://doi.org/10.5751/es-00015-010104

[23] Steyer, G.D., Sasser, C.E., Visser, J.M., Swenson, E.M., Nyman, J.A. and Raynie, R.C. (2003) A Proposed Coast-Wide Reference Monitoring System for Evaluating Wetland Restoration Trajectories in Louisiana: Environmental Monitoring and Assessment. In: Melzian, B.D., Engle, V., McAlister, M., Sandhu, S. and Eads, L.K. Eds., *Coastal Monitoring through Partnerships*, Springer, 107-117. https://doi.org/10.1007/978-94-017-0299-7_11

[24] Morton, R.A. and Barras, J.A. (2011) Hurricane Impacts on Coastal Wetlands: A Half-Century Record of Storm-Generated Features from Southern Louisiana. *Journal of Coastal Research*, **275**, 27-43. https://doi.org/10.2112/jcoastres-d-10-00185.1

[25] Barras, J.A. (2007) Satellite Images and Aerial Photographs of the Effects of Hurricanes Katrina and Rita on Coastal Louisiana. U.S. Geological Survey, Data Series 281. http://pubs.usgs.gov/ds/2007/281 https://doi.org/10.3133/ds281

[26] Lam, N.S.-N., Cheng, W., Zou, L. and Cai, H. (2018) Effects of Landscape Fragmentation on Land Loss. *Remote Sensing of Environment*, **209**, 253-262. https://doi.org/10.1016/j.rse.2017.12.034

[27] Stagg, C.L., Osland, M.J., Moon, J.A., Hall, C.T., Feher, L.C., Jones, W.R., *et al.* (2019) Quantifying Hydrologic Controls on Local- and Landscape-Scale Indicators of Coastal Wetland Loss. *Annals of Botany*, **125**, 365-376. https://doi.org/10.1093/aob/mcz144

[28] Potter, C. and Sukanna, T. (2023) Remote Sensing of Damage Inflicted on Coastal Wetlands of Southern Louisiana from Tropical Storms. *Journal of Coastal Research*, **40**, 235-245. https://doi.org/10.2112/jcoastres-d-23-00044.1

[29] Nyman, J.A., Carloss, M., Delaune, R.D. and Patrick, W.H. (1994) Erosion Rather than Plant Dieback as the Mechanism of Marsh Loss in an Estuarine Marsh. *Earth Surface Processes and Landforms*, **19**, 69-84. https://doi.org/10.1002/esp.3290190106

[30] Mariotti, G. (2016) Revisiting Salt Marsh Resilience to Sea Level Rise: Are Ponds Responsible for Permanent Land Loss? *Journal of Geophysical Research*: *Earth Surface*, **121**, 1391-1407. https://doi.org/10.1002/2016jf003900

[31] Ortiz, A.C., Roy, S. and Edmonds, D.A. (2017) Land Loss by Pond Expansion on the Mississippi River Delta Plain. *Geophysical Research Letters*, **44**, 3635-3642. https://doi.org/10.1002/2017gl073079

[32] Deis, D.R., Mendelssohn, I.A., Fleeger, J.W., Bourgoin, S.M. and Lin, Q. (2019) Legacy Effects of Hurricane Katrina Influenced Marsh Shoreline Erosion Following the *Deepwater Horizon* Oil Spill. *Science of The Total Environment*, **672**, 456-467. https://doi.org/10.1016/j.scitotenv.2019.04.023